

# Deformation Analysis of a Hummingbird Inspired MAV Flapping Wing using Digital Image Correlation

David Kumar,\* Akash Ravi Sharma, Tigmanshu Goyal, Vemuri Shyam, P M Mohite, Sudhir Kamle  
Department of Aerospace Engineering, Indian Institute of Technology Kanpur, India 208016

## ABSTRACT

Flapping wing micro air vehicles (MAVs) have the advantage of being able to fly at slow speeds and have high maneuverability. The design of a flapping wing MAV inspired by birds presents many technical challenges because birds as natural fliers exhibit higher efficiency than any man made flapping wing structure. Thus, the structure and motion of bird wings provide a starting point for the study of flapping wing MAV. In order to compare the deflections of the fabricated wings with the complex mechanism of the bird wings, it is required to quantify these deflections. Both the bird wings and the fabricated wings are very light weight and, therefore extremely light weight sensors or non-contact methods are required for the measurements of the deflections. Digital image correlation (DIC) provides one such option. DIC is an optical non-contact method used to acquire displacements. A simple two dimensional DIC code has been developed and validated in this work. Design and fabrication of wings is based on the hummingbirds. A 3D tapered wing design was developed and used for development of mold. This mold was used for fabrication of flexible polypropylene wings. For flapping motion measurements of wings, a simple slider-crank mechanism was designed to generate an oscillatory motion using brushless DC motors and Arduino Board. For modal analysis, an electrodynamic shaker was used to vibrate the wing with patterns stuck over its surface at its natural frequencies and captured the motion using a high speed camera. The captured images were analyzed using the developed DIC code and mode shapes for 1<sup>st</sup> and 2<sup>nd</sup> modes were obtained. For capturing the motion of a wing, a high speed camera mounted on a suitably designed stand was used. The validation of modal analysis was done using commercial finite element analysis software Ansys.

**Keywords:** MAVs, Digital Image Correlation, Hummingbirds, Modal Analysis.

## 1 INTRODUCTION

MAVs, small unmanned aircraft, can be used for surveillance, remote sensing, terrain mapping or reconnaissance operations. While they can be fixed wing, or rotary wing, flapping wing MAVs have the advantage of being able to fly at low speeds and have high maneuverability. The development of a flapping wing MAV presents many technical challenges. Some challenges include materials and structural aspects, low Reynolds number aerodynamics, weight and volume constraints, high propulsive power to weight ratio requirements and ability to adapt to all environments. Nature serves as an effective tool to study how MAVs should be operated. Natural Birds, the original masters of flight, use flapping wings to produce lift and thrust. They exhibit higher efficiency than any man made flapping wing structure. Thus, the structure and motion of their wings provide a starting point for the study of flapping wing MAV. Most birds are able to control their shoulder, elbow and wrist joints. Birds like hummingbird, however, can control only their shoulder joint but with more freedom and variety of motion providing them with the ability to fly in any direction and also hover, thus, making them highly maneuverable. The wing motion of birds can be broken down into flapping, pitching, lead lag and span reduction. Smaller birds use a combination of flapping, pitching and lead-lag while larger birds exhibit mostly flapping and span reduction. A combination of these motions along with the inherent flexibility and structure of the wings gives the birds the ability to generate lift and thrust. The flexibility of wings increases the aerodynamic efficiency of MAVs [1, 2]. Ansari et al [3] studied the motion of insect wing in hover and showed that the motion is in the shape of the figure of eight with the leading edge always leading i.e. the wing pitches so that the leading edge is always in forward motion. In order to understand the complex mechanism of the bird wings, it is required to quantify the deflections of the fabricated wings. The wings of smaller birds, like hummingbird, are very light weight and this prevents the placement of any heavy sensor on them as it will disrupt the weight distribution and add additional weight, which would be large in comparison to original weight of the wing. Extremely light weight sensors or non-contact methods are more effective in measuring the deflections. Digital Image Correlation provides one such option, it is an image registration technique used to measure deformations in two and three dimensions. It uses a series of images captured over a period of time to track and locate the displacement in desired features over the se-

\*Email address(es): david@iitk.ac.in

quence. Peters and Ranson [4] presented the technique for implementation in experimental stress analysis by measuring displacement of subsets of deformed surface images using intensity distributions. Sutton et al [5] gave an improvement to the method by suggesting a correlation coefficient based on minimizing the square of the difference between the chosen subset and all similar size subsets in the original array. Luo et al [6] extended the two dimensional DIC to three dimensions by using a pair of cameras along with a pin hole camera model and stereo imaging equations for transformation relating 3D world co-ordinates to 2D image co-ordinates. Tay et al [7] employed the pin hole camera model to determine the apparent change in in-plane displacement due to out of plane rotation and translation. The method however works for rigid motions only. Sutton et al [8] also studied the effect of out of plane motion on in-plane displacements in both 2D and stereovision 3D DIC, and compared the two along with the effects of using a telecentric lens. Even more recently Zhou and Chen [9] used the Zero Mean Normalized Sum of Squared Differences (ZNSSD) instead of the traditional Zero Mean Normalized Cross Correlation (ZNCC) for feature matching. Chen et al [10] used multiple camera system to obtain complete 3D information using stereovision system and the concept of point residual determination for the system of cameras. However, dependency on system setup, stability and calibration still remained in doubt. DIC was also used for MAV flapping wing analysis by Svanberg [11].

The objective of this work is to develop a DIC code that can be used to measure both in plane, out of plane deformations and mode shapes of the developed bio-inspired wing using only one camera. We try to obtain out of plane data by using only one camera along with co-ordinate transformation and a pin hole camera model. Along with the Correlation Coefficient, Fourier transform has been used to speed up the process of analyzing the acquired images in effort to take steps towards achieving live DIC processing. For the purpose of testing the developed code on flexible body motion, the hummingbird is chosen as the bio-inspiration for wing development and polypropylene is chosen as the wing material.

## 2 DIGITAL IMAGE CORRELATION TECHNIQUE

DIC is an optical non-contact method used to acquire displacements/strains of moving/deforming objects by tracking a unique distribution of pixel intensities of a grayscale image called as pattern or template. These patterns are correlated over a series of images of the object in concern to give the pixel displacement of the surface in the two dimensional images which can then be interpreted according to the three dimensional motion. It is therefore, highly useful when the object in consideration is not accessible, too small, too light, has variation in temperatures or is working at high speeds which prevent the use of traditional contact methods. Commonly, 2D DIC is used to measure in plane displacements. These are helpful in stress calculations and widely used in

experimental mechanics such as to study fractures. Generally two or more than two cameras are used in combination along with stereovision system principles in order to acquire three dimensional locations of points. Errors due to calibration of several cameras to function simultaneously, high precision required for the setup and the cost of obtaining several expensive high speed cameras for dynamic applications are some of its drawbacks.

### 2.1 Method Development

DIC uses the Correlation Coefficient, or the Correlation Coefficient with Fourier Transform which relies on tracking grayscale intensity values of image pixels in small neighborhoods called subsets or patterns.

#### 2.1.1 Correlation Coefficient

Correlation, given by Equation 1, is the normalized form of covariance. It is a dimensionless quantity and can be used to obtain relative strengths of relations between variables. Mathematically, for n observations of variables x and y,

$$Corr(x, y) = \frac{\sum_{i=1}^n (x - x')(y - y')}{\sqrt{\sum_{i=1}^n (x - x')^2 \sum_{i=1}^n (y - y')^2}} \quad (1)$$

Where,  $\bar{x}$  and  $\bar{y}$  are the means of x and y respectively.

The base of DIC technique lies with the Cross Correlation term. For any program, an input image is read as a matrix, where each pixel contributes to a value in the matrix. The value of this pixel comes from its grayscale intensity in the image. An image is hence, a 2D matrix of intensity values for the purpose of analysis. If  $f(x,y)$  is the base image (intensity function at x and y pixel locations) and  $t(x,y)$  is the feature or template, for displacements  $(u,v)$ , the measure of similarity between them is cross correlation (shown in Equation 2).

$$CCorr(u, v) = \sum_{x,y} [f(x, y)t(x - u, y - v)] \quad (2)$$

The cross correlation however, presents several disadvantages in term of using it in DIC. It is sensitive to the value of the image intensity of image and template. This arises a possibility that the correlation between the feature/template and a bright spot may be greater than the correlation with the actual match. In terms of practical application, it leads to high sensitivity to lighting conditions also, for the same reasons. The Normalized Cross Correlation term, given by Equation 3, or the Correlation Coefficient overcomes this difficulties by subtracting the mean of the image/template and by normalizing the image and feature vectors to unit length yielding a cosine like coefficient ranging from [-1 to 1] with the 1 being the perfect match.

$$NCCorr(u, v) = \frac{\sum_{x,y} [f(x,y) - f'(u,v)][t(x-u, y-v) - t']}{\sqrt{\sum_{x,y} [f(x,y) - f'(u,v)]^2 \sum_{x,y} [t(x-u, y-v) - t']^2}} \quad (3)$$

Where  $f'(u,v)$  is the mean intensity function of the image under the template and  $t'$  is the mean of the template.

### 2.1.2 Fast Fourier Transform

Fourier transform is a mathematical transform which provides one to one transform of signals from time domain to frequency domain. The Discrete Time Fourier Transform (DTFT) is Fourier Transform which receives discrete input in the time domain. This is helpful since in real applications, the signals we receive are discrete and do not have infinite points. The Discrete Fourier Transform (DFT), in addition to discrete time domain, is also discrete in the frequency domain. In 2D Fourier Transform of a image function  $f(x,y)$ , it is broken down into a linear combination of harmonic (sine, cosine etc) functions. The 2D Fourier can be computed line by line using 1D transform. The outcome is a function of complex variables. The Fast Fourier Transform is an efficient way to compute the Discrete Fourier Transform. The idea behind FFT is that a DFT of length  $N$  can be broken down into two DFTs of length  $N/2$ , first one consisting of odd samples and the second even samples. This means that any  $N$  length DFT can be broken down again and again till we get  $N/2$  number of 2 length DFTs. For  $N = 2^v$  this can be performed  $v = \lceil \log_2 N \rceil$  times. Thus the total numbers of multiplications reduce to  $N/2(\lceil \log_2 N \rceil)$  thereby giving a complexity of  $O(n \log(n))$ . As it has been established, that the frequency domain computation of the correlation term is faster in most cases, it would also be required to compute the normalization term or the denominator in the normalized cross correlation term (Equation 3) in frequency domain. This term can be computed easily using the method specified by JP Lewis [12]. It is computed using running sums of entire image first hand and then use them to calculate the mean and energy.

### 2.2 DIC Code Development and Validation

The DIC technique discussed was developed with the help of MATLAB software and was used to acquire back the applied known deviations and displacements. The purpose of these simulations was to help develop the code step by step, checking and verifying its accuracy and results along the process, before applying it to an experimental setup and finally concluding its feasibility for real world application. During simulations, firstly, one dimensional signals with and without noise were simulated and then extended to two dimensional matrices and images. Finally, a three dimensional rigid body simulation of a wing was performed. Here 3D rigid flapping wing simulation will be discussed.

#### 2.2.1 Pattern Development

Before going forward with 3D simulation of wing motions, it was essential to develop patterns with distinct intensity distributions which could be easily distinguished and identified by the DIC code. These patterns would be placed on the surface of the simulated wing and later printed and pasted on the actual wing. As the wing undergoes motion, the captured

images show an apparent movement of the surface points in two dimension. These patterns are placed on the surface and the DIC code used to capture these apparent two dimensional motions which are then interpreted in three dimensions. MATLAB reads image in the form of a grayscale matrix. Patterns of size 3x3 pixels were developed for use in simulation whereas the size was slightly larger for use in actual experimentation, 6x6 pixels (approximately 2mm x 2mm) to account for the blurring that would occur while printing and recapturing with a camera. The patterns were created with the help of commercial software Adobe Photoshop. Here are some examples of the patterns used. The variations in the

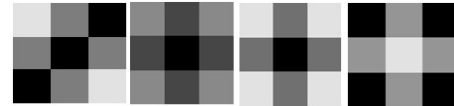


Figure 1: Sample patterns (3x3 pixels).

intensities form a unique pattern which can be matched by the correlation coefficient. For grayscale images, they vary from 0 for black to 255 for white and in between for shades of grey.

#### 2.2.2 3D Simulations

The motion of the bird wing generally consists of three major components, i.e. Flapping, Pitching and Lead Lag. Larger birds also exhibit reduction in span. Here, we try to simulate these three motion and recapture them through a series of images. The model of the wing used is same as that designed while manufacturing a bio-mimicking hummingbird wing. The Gambit model was exported to Autodesk 3ds Max. Autodesk 3ds Max is a 3D computer graphics software primarily used for realistic 3D animation and modeling. We use it to simulate simple rigid rotations about the three coordinate axis, with the patterns used for DIC recognition pasted onto its surface, and render the resulting animation into a series of images to be used in the developed code. The Figure 2 shows the typical rendered image of wing, with two different intensity patterns (x1 and x2) of the size 3x3 pixels, from the simulation upon which DIC code was run. The rendered image was of the size 2048x1556 but that

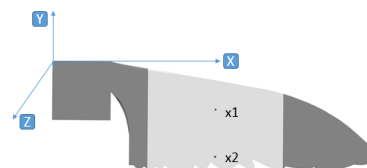


Figure 2: Sample 3D wing model with patterns (top view).

included the extents of the rendered viewport (here, top view

of the wing, as required for DIC), so the effective resolution covering the wing was lesser. Another point of note is that this rendering is not by a camera, i.e. this is not a camera image. There is no perspective projection here. It can be seen as a case of orthographic projection.

### 2.2.3 Simulation Results

The combined flapping, pitching and lead lag motion corresponds to the combination of out of plane and in-plane displacements i.e. motion about three different axis. Known excitation was given and the interpolated motion curve obtained from the 3ds Max software. The results, from DIC, were then compared with the simulation. Here, due to coupling of motion, one motion may affect the other. We used affine transformation equations to separate out individual components, as we obtained only the net displacement which is a sum of the displacements caused by all the motions. The Figure 3 shows the comparison of DIC results with the software generated motion curves at finite instants of the motion, called frames. The difference in the angles obtained from 3ds Max and the DIC code at each frame is the error.

For lead-lag or in-plane motion the results were found to lie

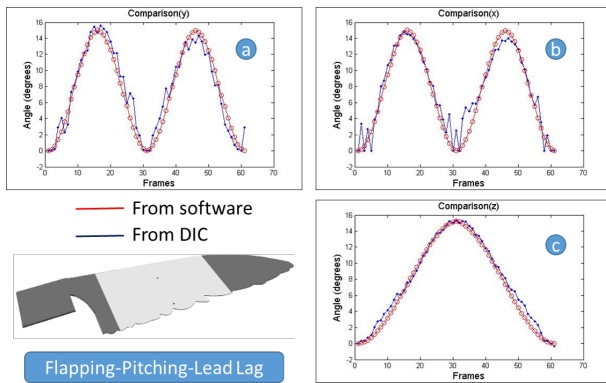


Figure 3: 3D wing simulation: (a) Flapping, (b) Pitching, (c) Lead Lag

in a low error range of 2%-5%, while for flapping and pitching cases the curves were found to deviate from actual response specially at lower angle values. The error obtained for the low angle regime lied in the range of 10%-25%. The simulations were also done for separate cases of flapping, pitching, lead lag. The errors for combined case are higher than in individual motion simulations because of the reflection of error in one term to another, but essentially the curves were replicated.

## 3 WING DEVELOPMENT AND EXPERIMENTAL SETUP

In this section we discuss the development procedure of a bio-inspired hummingbird wing. Polypropylene, a thermo-

plastic semi rigid polymer, is chosen as the wing material because along with light weight it has good fatigue resistance, flexibility, mechanical strength, toughness, heat and chemical resistance, etc. Developed DIC code is used with dynamic testing experiments of fabricated wings. A high speed camera with a developed flapping mechanism as well as an electrodynamic shaker is used for performing experiments.

### 3.1 Wing Design and Fabrication

For the development of a successful flapping wing MAV, it is essential that the wings be light, able to flap at high flapping frequencies and amplitude, structurally strong and aerodynamically efficient. In order to make wings with such characteristics we choose hummingbirds as bio-inspiration. The dimensions and other characteristics of the giant hummingbird are taken as the starting point for designing the wing. The Table 1 shows the characteristics of Giant Hummingbird.

The wing was developed using commercial software Gam-

| Parameter                        | Giant Hummingbird |
|----------------------------------|-------------------|
| Body Mass ( <i>gm</i> )          | 18-24             |
| Wing Length ( <i>mm</i> )        | ~135              |
| Wing Chord ( <i>mm</i> )         | ~45               |
| Flapping Frequency ( <i>Hz</i> ) | 10-15             |
| Top speed ( <i>km/h</i> )        | ~43.44            |

Table 1: Giant hummingbird characteristics

bit, using a matching wing structure to the actual wing. Using a detailed and accurate image of the wing, the dimensions are accurately recorded with a digitizer. The same data points were used to replicate the structure in Gambit. The wing design was validated using the plots and equations providing relations between wing length, area and bird weight by Greenewalt [13]. The length of designed wing is 113.8 *mm*. The total wing surface area calculated using Greenewalt Equation 4, for current wing length as reference, is 7222 *mm*<sup>2</sup> which is close to current total wing area 6932 *mm*<sup>2</sup>.

$$L = 1.0537S^{0.5556} \quad (4)$$

where L and S are in cm and *cm*<sup>2</sup> respectively. The designed wing sketch was extended to a both side tapered simple solid model. The thickness was varied from shoulder (1.2 *mm*) to tip (0.5 *mm*).

The repeatability is one of the key factors of manufacturing techniques. One must be able to manufacture the same object with same properties repeatedly. Here, we need at least two wings for MAV application and with same characteristics to avoid uncontrolled asymmetric flapping. A mold was designed to cast the desired wing. The mold for the polypropylene wing was made out of brass from the 3-Axis CNC machine. For fabrication of wings the mold, with the material within it, was put in the thermal chamber of UTM in compression mode. The temperature of chamber was set up to 230-

240 degC. The molds are compressed till they completely fit as designed. Final fabricated wing is shown in Figure 4.

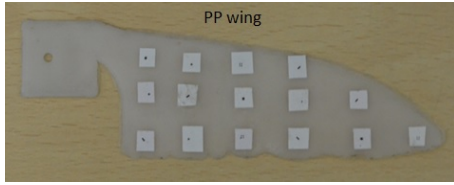


Figure 4: Polypropylene wing with patterns for DIC analysis.

### 3.2 Experimental Setup

The developed DIC code is used to measure both in plane & out of plane deformations and mode shapes of the developed bio-inspired wing using only one camera. Out of plane displacement data was obtained using co-ordinate transformation. Fourier transform has been used along with Correlation Coefficient to speed up the process of analyzing the acquired images. A high speed camera, Olympus i-SPEED TR, is used for capturing images of the moving wing. It supports a maximum resolution of 1280x1024 pixels till 2000 *fps*. Since it is required to capture the surface of the wing, an appropriate stand was designed to hold the camera safely and in a stable position. DIC requires a speckle pattern as it correlates the high contrast pixel intensities from one image (reference image) to the other image (template image). A black and white speckled pattern is required for a proper correlation. The patterns were attached on the surface of the wing, as discussed in 2.2.1. These patterns were used to depict the displacements of their corresponding sections of the wing.

#### 3.2.1 Wing Motion Measurement Setup

For measurements of wing motion, a motor assembly was designed to provide a flapping motion to the attached wing. The designing process was carried out in commercial software SolidWorks. Each part of the mechanism was separately modeled and assembled. The manufacturing was carried out using FDM Rapid Prototype machine. The manufactured flapping mechanism with high speed camera and setup is shown in the Figure 5.

#### 3.2.2 Modal Analysis Setups

For modal analysis of wings, the electromagnetic shaker is used to vibrate the wing. The natural frequencies were obtained by observing the deflections of vibrating wing through stroboscope and laser displacement sensor. The stroboscope visually shows the nature of mode shapes. For measuring nature of mode shapes using DIC, for 1<sup>st</sup> and 2<sup>nd</sup> modes, high speed camera used for recording frames of vibrating wing.

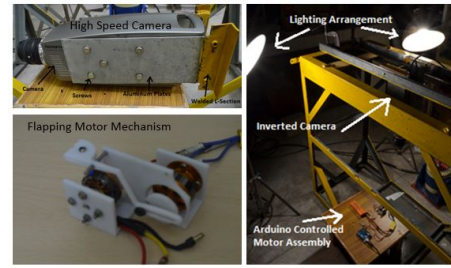


Figure 5: Flapping wing motion measurement setup.

The set-up is shown in Figure 6.

Two 500 Watt bulbs were used as light sources for both the

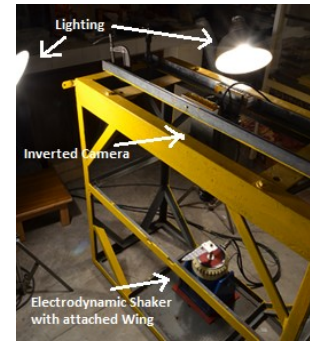


Figure 6: Modal analysis setup.

analysis.

### 3.3 Modal Analysis Results and Validation using Ansys

The natural frequency and mode shapes of wing were determined with the help of stroboscope and laser displacement sensor. The fundamental natural frequency mode comes at 19 *Hz* and second mode at 78 *Hz*.

To obtain the modal frequencies and mode shapes using Ansys, a three dimensional model of the wing was analyzed using the Modal Analysis module. First the material data for PP was entered, and then solid three dimensional model, made using Gambit software was imported. The dimensions of the model were the same as that of the manufactured polypropylene wing. The model was given a fixed support at its shoulder joint. Meshing was done using patch conforming method with tetrahedrons elements (Figure 7 (a)). The input material

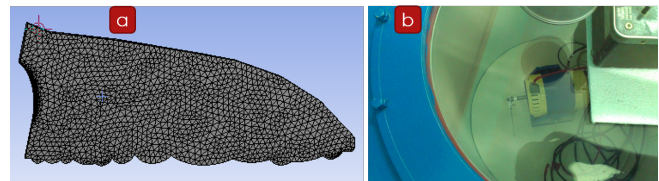


Figure 7: Wing modal analysis: (a) Meshed wing, (b) Wing in vacuum chamber

data (Density =  $901 \text{ kg/m}^3$ , Modulus =  $1.16 \text{ GPa}$ , Poisson's ratio = 0.45) except Poisson's ratio, given for PP wing analysis, was obtained through PP film development and testing. The free un-damped vibration case was taken for solving the problem. In actual case the wing is subjected to two types of damping. One due to system or viscoelastic nature of wing material and second due to fluid or air interaction. A vacuum chamber was designed, developed and used for wing testing (Figure 7 (b)). Using vacuum chamber the contribution of fluid damping (due to air resistance) can be eliminated. Therefore, for validation of experiments, the results from Ansys are compared with vacuum testing results.

#### 4 RESULTS AND DISCUSSION

Here, the results of the dynamic testing of the developed polypropylene wings are discussed.

##### 4.1 Flapping Motion Measurements Results

We use flapping mechanism which was run by the Arduino micro-controller board and capture the motion via the high speed camera at 750fps with f/8 aperture settings. The angles were noted along 4 points on the wing span, point 4 being nearest to the shoulder and point 1 nearest to the tip of the wing. Their respective distances from the shoulder being 10 mm, 35 mm, 60 mm and 85 mm for point 4, 3, 2 and 1. As this can be seen from Figure 8, at point 4 which is nearest to the shoulder, the deflections are lesser as compared to the one farther away because of the bending of the wing. Maximum out of plane motion at point 4 is approximately  $21.6^\circ$ , at point 3 it is  $24.7^\circ$ , at point 2 it is  $30.8^\circ$  and farthest away, at point 1,  $34.6^\circ$ .

The clump of zeros between transition from out of plane to in

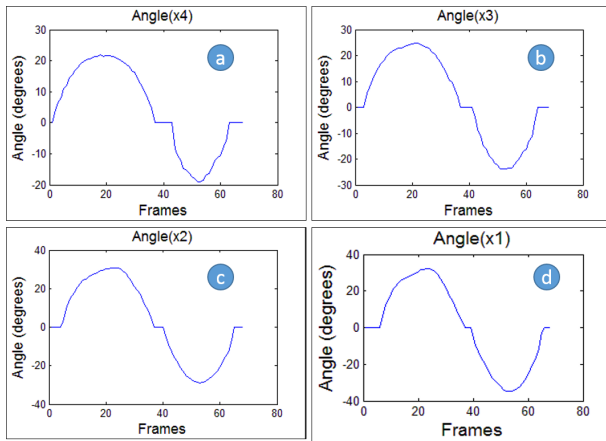


Figure 8: Angles versus Frames at (a) point 4 (b) point 3 (c) point 2 (d) point 1

plane represent the points where angles are small, here taken to be zero. It can also be seen that the point nearest to the shoulder, i.e., point 4 has the largest span of the small angle values which are not captured as the speed along this point

is slower. As we go farther down the span, the speed of the point increases and the number of frames in the range of the small angles which are not interpreted decreases. Also, there is a lag in the cycle with the farther points lagging slightly behind the points nearer to the shoulder of the wing and hence the axis of rotation because of bending.

##### 4.2 Experimental and Computational Modal Analysis Results

The results of modal analysis done in Ansys and vacuum (Table 2) do not match because of two reasons, one is that the un-damped vibration case was solved for the wing and second, may be due to experimental wing development and testing errors. Damping characteristics of wing material, PP, have not been obtained in the present study. The dynamic characterization of wing material using dynamic mechanical analysis can be done to obtain the damping characteristics. The damping characteristics of wing material can be given in Ansys for solving damped vibration case which will decrease the difference between computational and experimental results.

| Modes           | in Air | in Vacuum | Ansys | Mode shape |
|-----------------|--------|-----------|-------|------------|
| 1 <sup>st</sup> | 19     | 19        | 17.2  | Bending    |
| 2 <sup>nd</sup> | 78     | 78        | 70    | Coupled    |
| 3 <sup>rd</sup> | 124    | 124       | 94.5  | Torsional  |

Table 2: Modal analysis results: Natural frequencies.

Another point to note here is that, from Table 2, the natural frequency values are same from both vacuum and normal atmospheric testing conditions. This is because of a very small surface area and relatively stiff structure of wing for any significant air interaction to occur. Hence the damping due to air does not affect the modal frequencies of this particular wing. So it can be concluded that the aerodynamic loading or air interaction, for the wing designed in present study, does not affect the mode frequencies (at least for first three measured modes). For a more flexible wing in comparison to current wing the natural frequency and wing deflection should increase. Chakravarty [14] did modal analysis on hyperelastic membrane. He found that the natural frequency, with very small change, and deflections increase in vacuum. In present study the mode shapes have not been measured in vacuum. To separate the forces generated by wing during flapping can be done by measuring the forces using force balance in air and vacuum followed by subtraction of forces in vacuum from total force in air.

##### 4.3 Mode Shapes Measured using DIC

For first fundamental frequency or resonance mode, the patterns were stuck along the span of the polypropylene wing to note the displacements along the span. They were placed at known distances in two separate lines as shown in Figure 9

(a), line 1 and line 2.

The setup was run at 19 Hz at suitable qualitative ampli-

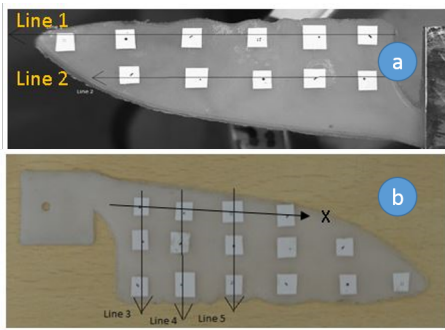


Figure 9: Lines on the wing: (a) Lines along the span of wing , (b) Lines along span and chord of wing

tude and recorded via the high speed camera at 200 fps with aperture set at f/8. At 200 fps, 19 Hz corresponds to 10.52 frames per cycle. The Figure 10 shows that the mode shapes

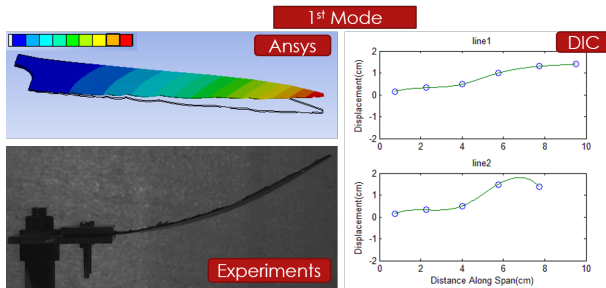


Figure 10: 1<sup>st</sup> mode

from Ansys, DIC and experiments are similar (where line 1 and line 2 for DIC results corresponds to the lines shown in Figure 9 (a)).

For second mode a third line X, shown in Figure 9 (b), of patterns were placed to provide an additional point to get the twisting nature of coupled mode. The setup was run at 78 Hz (second mode frequency) and vibrating wing motion was recorded at 1000 fps. The nature of mode shapes are compared, Figure 11. Mode shapes are similar which validate DIC code and Ansys results. This mode is coupled in nature because the tail part deflections are higher than leading edge deflections of wing.

#### 4.4 Wing-tip Displacement Response

The objective of this study is to determine the relation between wing-tip response and wing-root excitation. The wing was attached to the electromagnetic shaker and excited at different root amplitudes for first resonance mode. The displacements of wing-tip and wing-root were measured using laser displacement sensor with NI-DAQ cards. The Equation 5 shows the proportionality between wing-tip response and

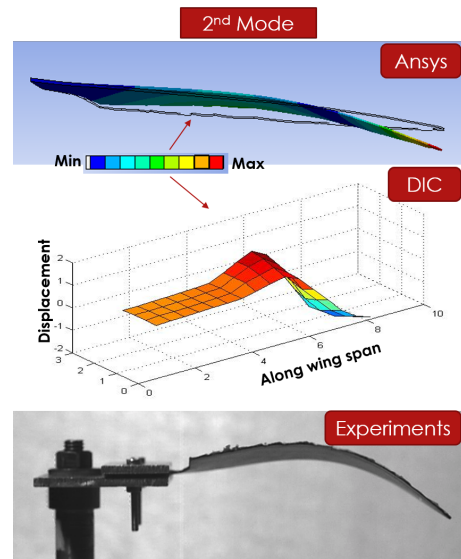


Figure 11: 2<sup>nd</sup> mode

wing-root excitation as obtained from Figure 12 (d).

$$Y_{tip} = 13.1 * Y_{root} \quad (5)$$

where  $Y_{tip}$ ,  $Y_{root}$  are wing-tip and wing-root displacements respectively. The experimental setup and results for this analysis are shown in Figure 12.

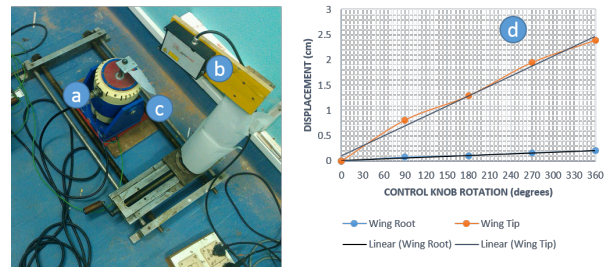


Figure 12: Wing-tip response: (a) Electromagnetic shaker, (b) Laser displacement sensor, (c) Wing, (d) Results

## 5 CONCLUSION

The aim of this study was to develop a non-contact method to study the fabricated hummingbird inspired wing deformations. DIC was chosen as the suitable method. Firstly, the fundamentals of Correlation and Frequency domain analysis using Fourier Transform were established. A DIC code was developed with the help of MATLAB based on capturing a designed template with unique grayscale intensity distribution. Simulations were carried out to validate the developed code. Patterns of size 3x3 pixels were developed for use in rigid body simulations. Rigid body simulation of a hummingbird

wing was carried out. High errors were consistently seen for small angles of rotation less than  $2^\circ$ . However, they reduced drastically for angles larger than  $2^\circ$  and stayed less than 5 % for nearly all cases. The results were better for in plane motions than out of plane motions. Error was also seen to be dependent on proximity with the axis of rotation. For the combined motions, errors obtained were higher because of the error in one term being reflected in the other.

For experimental application, DIC code was used for measurements of flexible body motion, design and fabrication of wings based on the Hummingbird. The wings were made of polypropylene. A simple slider-crank mechanism was designed to generate an oscillatory motion using brushless DC motors and Arduino Board. For capturing the motion, a high speed camera mounted on a suitably designed stand was used. The captured images were analyzed using the developed DIC code and the flapping motion was obtained. An electromagnetic shaker was used to vibrate the wing. The first and second modes were determined using stroboscope and laser displacement sensor. The three dimensional model of the wing was analyzed through Ansys modal analysis to validate the experimental results. The natural frequencies values from Ansys were compared with experimental modal analysis values of wing in vacuum chamber. The high speed camera was used to record the vibrating motion of wing (with patterns). The stored images were analyzed using DIC code for determining the mode shapes which were compared with experimental and Ansys mode shapes. The mode shapes (from DIC, Ansys and Experiments) were found to be similar. It was therefore found that the developed DIC code was a reliable method to analyze flapping wing deformations, which were then studied to mimic the Hummingbird wing motions with a reasonable accuracy.

#### ACKNOWLEDGEMENTS

We would like to acknowledge the support of the following departments from IIT Kanpur: ME (4i lab), AE (workshop and structures lab) and MSE. We also thank NP-MICAV, India.

#### REFERENCES

- [1] S. Heathcote, Z. Wang, and I. Gursul. Effect of span-wise flexibility on flapping wing propulsion. *Journal of Fluids and Structures*, 24(2):183 – 199, 2008.
- [2] Y. WenQing, S. BiFeng, S. WenPing, and W. LiGuang. The effects of span-wise and chord-wise flexibility on the aerodynamic performance of micro flapping-wing. *Chinese Science Bulletin*, 57(22):2887–2897, 2012.
- [3] S.A. Ansari, R. bikowski, and K. Knowles. Aerodynamic modelling of insect-like flapping flight for micro air vehicles. *Progress in Aerospace Sciences*, 42(2):129 – 172, 2006.
- [4] W.H. Peters and W.F. Ranson. Digital imaging techniques in experimental stress analysis. *Optical Engineering*, 21(3):213427–213427, 1982.
- [5] M.A. Sutton, W.J. Wolters, W.H. Peters, W.F. Ranson, and S.R. McNeill. Determination of displacements using an improved digital correlation method. *Image and Vision Computing*, 1(3):133 – 139, 1983.
- [6] P. F. Luo, Y.J. Chao, M.A. Sutton, and W.H. PetersIII. Accurate measurement of three-dimensional deformations in deformable and rigid bodies using computer vision. *Experimental Mechanics*, 33(2):123–132, 1992.
- [7] C.J. Tay, C. Quan, Y.H. Huang, and Y. Fu. Digital image correlation for whole field out-of-plane displacement measurement using a single camera. *Optics Communications*, 251(13):23 – 36, 2005.
- [8] M.A. Sutton, J.H. Yan, V. Tiwari, H.W. Schreier, and J.J. Orteu. The effect of out-of-plane motion on 2d and 3d digital image correlation measurements. *Optics and Lasers in Engineering*, 46(10):746–757, 2008.
- [9] Y. Zhou and Y.Q. Chen. Feature matching for automated and reliable initialization in three-dimensional digital image correlation. *Optics and Lasers in Engineering*, 51(3):213–223, 2013.
- [10] F. Chen, X. Chen, X. Xie, X. Feng, and L. Yang. Full-field 3d measurement using multi-camera digital image correlation system. *Optics and Lasers in Engineering*, 51(9):1044–1052, 2013.
- [11] C.E. Svanberg. *Biomimetic micro air vehicle testing development and small scale flapping wing analysis*. Air Force Institute of Technology, Wright Patterson Air Force Base, Ohio, Ohio, 2008.
- [12] J.P. Lewis. Fast normalized cross-correlation, 1995.
- [13] C.H. Greenewalt. *The flight of birds : the significant dimensions, their departure from the requirements for dimensional similarity, and the effect on flight aerodynamics of that departure*. American Philosophical Society, Philadelphia, 1975.
- [14] U.K. Chakravarty. Analytical and finite element modal analysis of a hyperelastic membrane for micro air vehicle wings. *Journal of Vibration and Acoustics*, 135(5):051004, 2013.